Pergamon

Journal of Structural Geology, Vol. 20, No. 4, pp. 355 to 362, 1998

0191-8141/98 $19.00 + 0.00

PII: 0191-8141(97)00090-4

Extensional layer-parallel shear and normal faulting

DAVID A. FERRILL

Center for Nuclear Waste Regulatory Analyses, Southwest Research Institute, 6220 Culebra Road, San Antonio, TX 78238, U.S.A.

ALAN P. MORRIS

Division of Earth and Physical Sciences, University of Texas at San Antonio, San Antonio, TX 78249, U.S.A.

SIDNEY M. JONES and JOHN A. STAMATAKOS

Center for Nuclear Waste Regulatory Analyses, Southwest Research Institute, 6220 Culebra Road, San Antonio, TX 78238, U.S.A.

(*Received* 6 *May* 1997; *accepted in revised form* 21 *September* 1997)

Abstract—An extensional fault system in Bare Mountain, Nevada, U.S.A., contains abundant evidence of layer-parallel shear deformation contemporaneous with faulting. Layer-parallel shear is manifest by deformation of pre-faulting fabrics and cleavage at low angles to bedding that indicate shear in the down-dip direction, perpendicular to fault–bedding intersections. Layer-parallel shear along discrete bedding planes locally offsets normal faults, and shear distributed within layers reorients block-bounding normal faults. In simple rigid block models of extension accommodated by normal faults above a low-angle detachment or décollement, extension causes faults to rotate to progressively shallower dips, while originally horizontal beds rotate to steeper dips. These rotations reorient faults out of originally optimum conditions for slip into orientations of a lower slip tendency, whereas bedding rotates to steeper dips with progressively higher slip tendency. The timing or amount of rotation before the initiation of layer-parallel shear depends on the frictional resistance to sliding or resistance to shearing within layering in fault blocks. Offset or deflection of block-bounding normal faults may cause faults to lock as extension increases. Alternatively, bedding and faults may become simultaneously active, progressively lowering dips of faults and bedding until neither is well oriented for slip, at which point new faults are required to accommodate additional extension. At Bare Mountain, early extension within the fault system was accomplished by fault slip and associated block rotation. Continued extension took place by slip along bedding within fault blocks.

INTRODUCTION

Extensional imbricate fault systems consisting of several nearly parallel normal faults ("domino" or "bookshelf" faulting) are relatively common in regions of extensional deformation. Examples include unlithified sedimentary strata in the Gulf of Mexico (Diegel *et al.*, 1995), sedimentary strata in the North Sea (Rouby *et al.*, 1996), and sedimentary and volcanic strata in the Basin and Range province (Anderson, 1971; Wernicke and Burchfiel, 1982; Maldonado, 1990). Displacement in these systems is linked either by faults that merge downward into a low-angle detachment, or by transfer of fault displacement downward into a thick décollement zone (Fig. 1) (Brun and Choukroune, 1983). Faults in extensional imbricate systems are assumed to typically form with steep dips (around 60°) representing optimal failure orientations in a normal faulting stress regime (Anderson, 1951). Fault blocks are commonly assumed to rotate rigidly with negligible internal deformation during progressive extension (e.g. Proffett, 1977; Wernicke and Burchfiel, 1982).

Other deformation mechanisms inferred to operate in extensional settings are vertical simple shear and oblique simple shear (e.g. Dula, 1990; Groshong, 1990), which require constant thickness parallel to the shear direction, and layer-parallel shear, which assumes constant bed length and thickness (Suppe, 1983; Ferrill and Morris, 1997). Vertical and oblique simple shear algorithms are the most widely used in cross-section construction and restoration, although Higgs *et al.* (1991) recognized evidence of layer-parallel simple shear associated with natural extensional faulting. Of these mechanisms, only constant bed length and thickness deformation above steep (>60°) but downward flattening normal faults involves a component of down-dip, layer-parallel shear in the hangingwall (Higgs *et al.*, 1991; Ferrill and Morris, 1997).

In this paper we explore an imbricate fault system exposed in profile at Bare Mountain, in the western Basin and Range of Nevada, as a natural example of deformation mechanisms in extensional fault systems. Fault blocks in this system display a variety of structures indicating internal deformation by layer-parallel shear with displacement top-towards-the-fault and down-dip. We use slip tendency analysis (Morris *et al.*, 1996) to interpret the sequence of deformation during fault displacement, which reinforces our interpretations

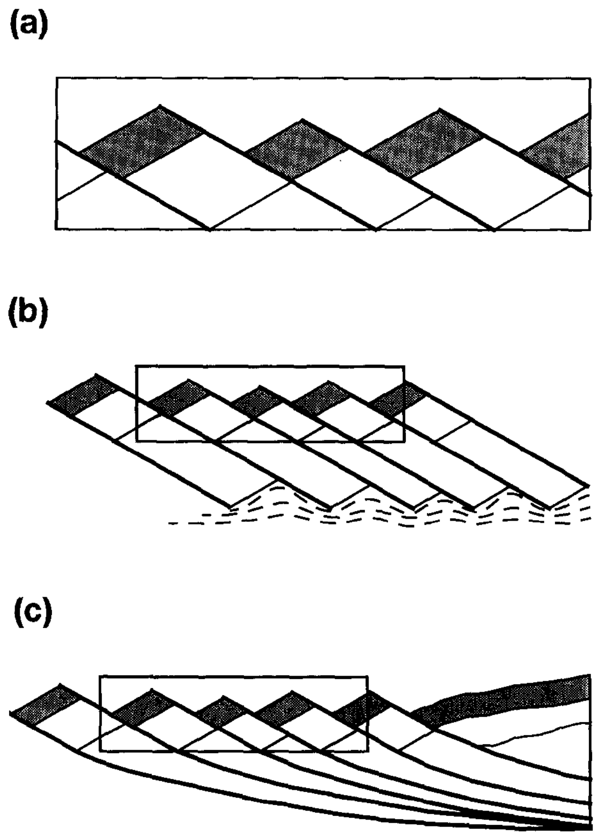

Fig. 1. Schematic illustration of imbricate normal fault systems (a) in which fault blocks rotate above either (b) a thick décollement horizon or (c) a detachment surface. Rectangular box in (b) and (c) marks area shown in (a).

of the structural style observed at Bare Mountain. Based on these results, field observations and geometrical considerations, we describe five characteristics of layer-parallel shear in extensional fault systems: (1) extensional layer-parallel shear is characterized by a down-dip sense of shear, opposite to that observed in contractional structures; (2) non-uniformly distributed extensional layer-parallel shear strain tends to be concentrated in weak layers or along layer boundaries, similar to layer-parallel shear in compressional settings (e.g. Ferrill and Dunne, 1989); (3) increasing extension and steepening of stratal dips in extensional fault blocks tends to increase down-dip layer-parallel shear relative to slip on faults; (4) increasing extension rotates faults and fault blocks into orientations more favorable for layer-parallel shear and less favorable for fault slip; and (5) extensional layer-parallel shear progressively rotates layering within fault blocks to lower dips.

EFFECTS OF STRESS FIELD ON PROGRESSIVE DEFORMATION

Early models of imbricate normal faulting treated fault blocks as rigid bodies that progressively rotate during deformation (e.g. Proffett, 1977; Wernicke and Burchfiel, 1982). Initially, layering is typically subhorizontal and faults dip steeply. In a typical normal faulting stress regime, where the maximum principal compressive stress (σ_1) is vertical, the resolved normal stress (σ_n) on horizontal bedding is equal to σ_1, and resolved shear stress (τ) is zero. Therefore, initial slip tendency (τ/σ_n) for horizontal bedding is zero. In contrast, 60°–70° normal faults have large resolved shear stress and small resolved normal stress. Therefore, the slip tendency of high-angle normal faults is initially at or near the maximum possible in the stress field.

In our model, fault blocks rotate with progressive extension, bedding rotates to steeper dips and faults rotate to shallower dips. The tendency for slip on bedding increases and the tendency for slip on faults decreases with increasing extension and block rotation. Given equal frictional resistance to sliding (μ) on faults and bedding, slip on bedding would begin to accommodate extension as bedding is rotated to dip more steeply than faults. For example, a situation in which faults initiate at 60° in horizontal strata, with frictional resistance to sliding equal for bedding and faults, and fault blocks that initially rotate rigidly, will yield equal slip tendencies for faults and bedding once faults and bedding both dip at 30° (Fig. 2). As extension continues, slip on the normal faults rotates faults to even lower dips, and down-dip slip on bedding simultaneously rotates bedding to lower dips within fault blocks. At large extensions, neither faults nor bedding are likely to be appropriately oriented for slip, at which time new faults form to accommodate additional extension (Proffett, 1977; Ramsay and Huber, 1987, p. 518).

The actual occurrence of slip on a fault or bedding surface depends on frictional resistance to sliding and cohesion on the surface, and other complications such as intersections of slip surfaces that might lock. In some cases, resistance to sliding on bedding or shear within layers may be lower than frictional resistance to sliding on faults, because of the presence of weak horizons that slip or plastically deform easily. Therefore, weak horizons may slip or shear at relatively low slip tendencies.

EXTENSIONAL FAULTING AT BARE MOUNTAIN, NEVADA

Bare Mountain is an extended and uplifted block of Precambrian and Paleozoic strata exposed in southwestern Nevada (Fig. 3). The block is bounded on the east by the Bare Mountain fault, a steeply E-dipping normal fault that has been active since the Middle Miocene (e.g. Ferrill *et al.*, 1996a, 1997). Bare Mountain is also in the footwall of the Fluorspar Canyon–Bullfrog Hills detachment system that was also active during the Middle Miocene (Maldonado,

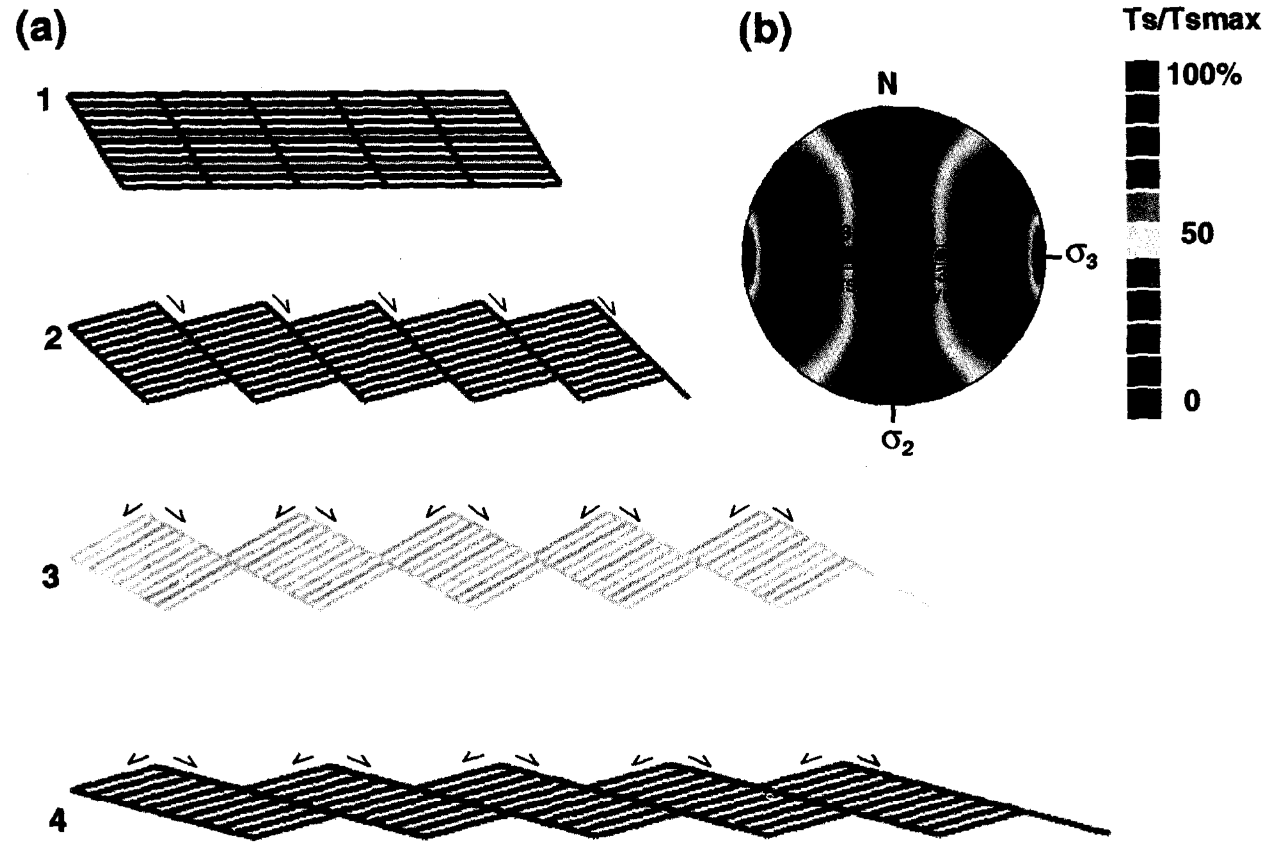

Fig. 2. (a) Slip tendency analysis of domino faults and layering within fault blocks during progressive extension. Slip tendency (T_S) is the ratio of shear stress (τ) to normal stress (σ_n) resolved on a surface ($T_S = \tau/\sigma_n$), described by Morris *et al.* (1996), within a given stress field. Colors and numbered fault- and bedding-poles in (b) correspond to faults and bedding represented in profiles in (a). (b) Lower-hemisphere equal-angle stereographic projection illustrating slip tendency distribution for faults in a typical extensional stress regime. Conceptual rotation paths of faults and bedding (layering) within the stress field during progressive deformation are also shown.

1990). Lateral variations of stratigraphic age and metamorphism of exposed strata, and pre-Middle Miocene (Oligocene?) structures exposed in the central part of

Fig. 3. Location map and latitude and longitude coordinates of the Gold Ace Mine fault system at Bare Mountain, southwestern Nevada (see Fig. 4).

Bare Mountain, indicate a NE plunge for major structural elements of the range. Consequently, the steep southwestern flank of the mountain now exposes a profile nearly perpendicular to the plunge of the range. This profile reveals a pre-Middle Miocene extensional fault system consisting of presently E-dipping normal faults (Fig. 4), which we interpret as an originally SE-dipping fault system that was subsequently rotated to its present orientation during later Tertiary NE tilting of the Bare Mountain block (Ferrill *et al.*, 1996b; Stamatakos and Ferrill, 1996). Of these normal faults, the Gold Ace Mine fault has the largest displacement, with nearly 3 km of stratigraphic separation. An outcrop of the hangingwall of the Gold Ace Mine fault exposes a meso-scale extensional imbricate fault system (Fig. 4) consisting of E-dipping, curved, normal faults that offset N-dipping Cambrian limestones and dolomites. Bedding–fault cut-off angles are typically 50°–60° and the cut-off lines plunge NE. Faults are approximately 10–100 m apart with displacements of 5–75 m. Strata in the Gold Ace Mine exposure (shown in Fig. 4) are dominantly the Papoose Lake Member of the Bonanza King Formation and consist of white–dark gray limestone and dolomite, with sparse intercalated yellowish-orange silty and sandy beds (Monsen

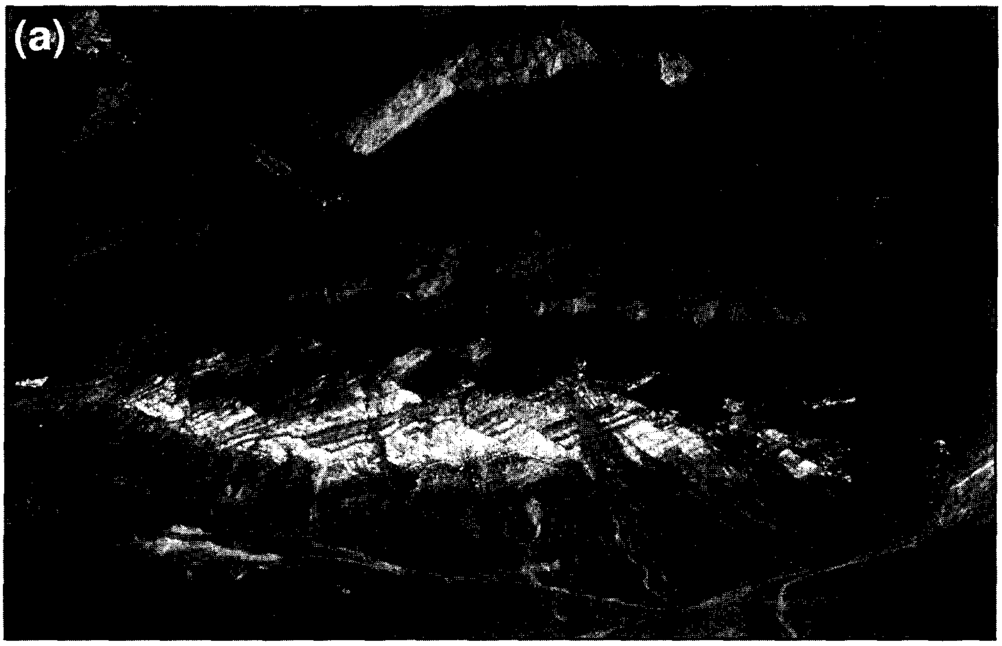

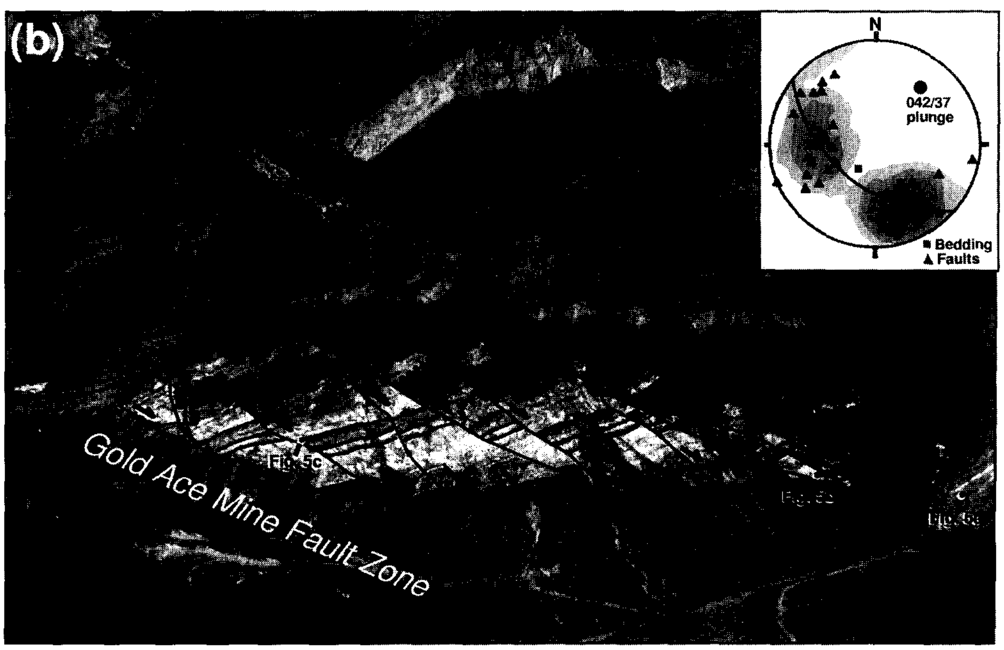

Fig. 4. (a) Uninterpreted and (b) interpreted oblique aerial photograph of normal fault system (in the hangingwall of the Gold Ace Mine fault zone) exposed in the southwestern side of Bare Mountain, Nevada. View is looking down and to the northeast. Width of field of view is approximately 0.6 km.

et al., 1992). The lowermost part of the outcrop exposes the basal contact of the Bonanza King Formation, and underlying medium gray limestone of the upper part of the Carrara Formation.

Deformation within fault blocks at the Gold Ace Mine exposure is manifest by a range of microscopic to mesoscopic structures, spans the spectrum of behavior from ductile to brittle and is inhomogeneously distributed. High-amplitude, bedding-parallel stylolites are common and frequently exhibit a strong pattern of stylolitic teeth inclined to bedding that indicate layer-parallel shear with a top toward the underlying fault (down-dip) sense, and angular shear magnitudes of more than 45° (Fig. 5a). Predominantly recrystallized, fossiliferous and oolitic limestones display a penetrative shape alignment fabric (defined by elliptical grain shapes) consistent with a down-dip shear sense. Spaced cleavage at a low angle (< 45°) to bedding, in rare thin argillaceous limestone beds, also verges in the down-dip direction (Fig. 5c), which suggests active pressure solution during down-dip layer-parallel shear. Thin, localized, slip zones composed of anastomosing sys-

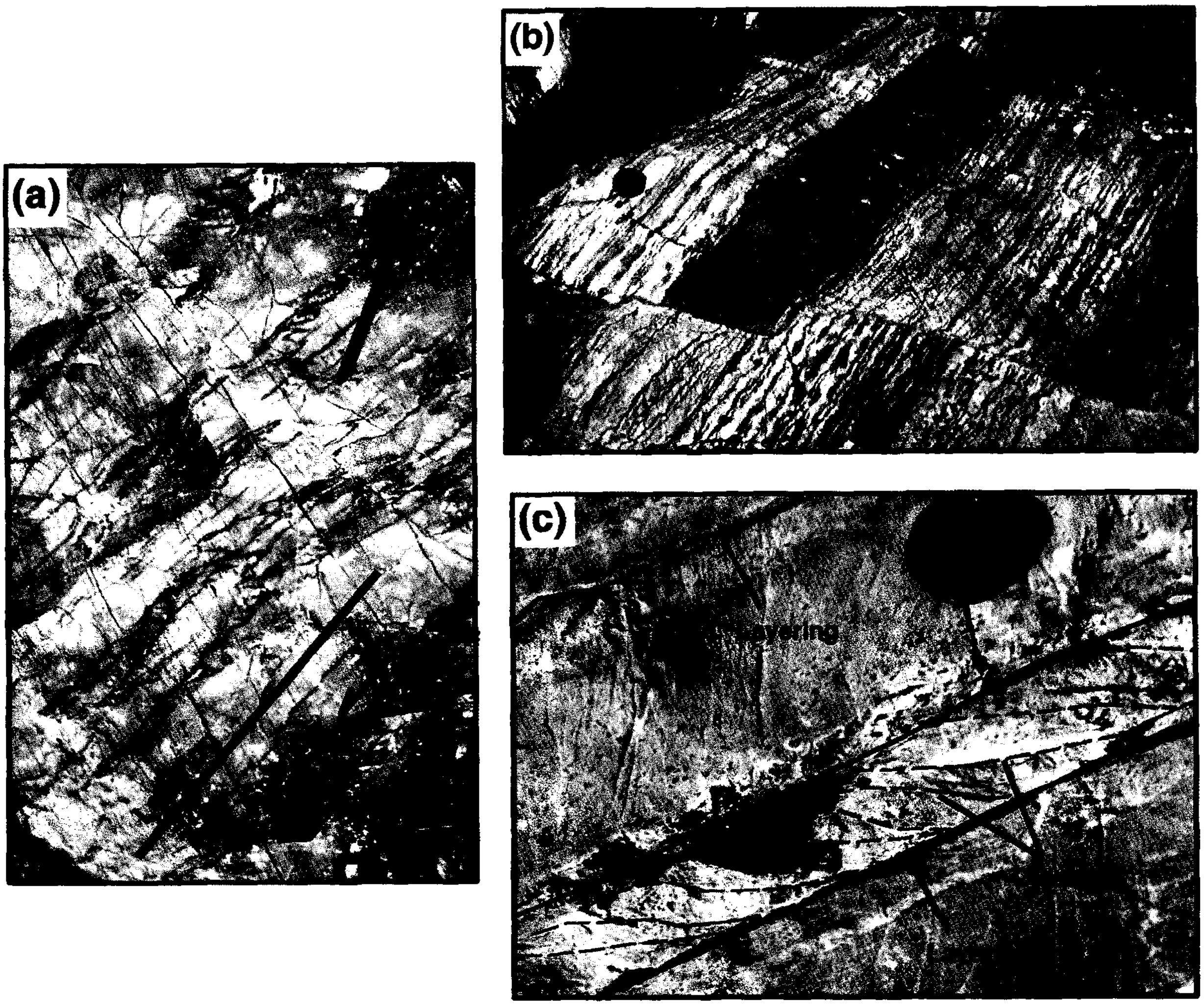

Fig. 5. Photographs of (a) stylolite teeth deformed by layer-parallel shear distributed through carbonate layer, (b) normal fault offset by extensional layer-parallel slip along bedding and (c) cleavage oblique to bedding, consistent with down-dip sense of shear. Locations where photographs were taken are shown in Fig. 4(b).

tems of discrete slip surfaces are common between relatively stiff sandy or silty beds and weaker limestone beds. Some of these zones clearly offset block-bounding normal faults (Fig. 5b), indicating that layer-parallel shear post-dates slip on at least some of the normal faults.

SLIP TENDENCY ANALYSIS OF FAULTS AT BARE MOUNTAIN

To evaluate the described pattern of fault slip and internal deformation in the context of resolved stresses on faults and bedding during fault system development, we first mapped the Gold Ace Mine exposure using a plane table and alidade. This map provided us with detailed geometric data on the fault system and allowed us to construct a down-plunge profile. Fault and bedding orientations were collected throughout the mapped area and were used to define the plunge of the fault–bedding intersection at the exposure (Fig. 4b). A plunge-perpendicular cross-section was then generated by projecting all structural data onto a plane normal to the fault–bedding intersection line (Fig. 6). In this cross-section, faults dip 20°–65° to the SE, and bedding dips 15°–65° to the NW. We consider this cross-section to represent the fault system geometry at the end of its period of activity and prior to the NE tilting of the Bare Mountain block.

The *pattern* of relative slip tendency is sensitive to orientations and relative magnitudes of the principal stresses that define the stress tensor, and less sensitive to the actual magnitudes of the principal stresses. We have no detailed constraints on the stress field during faulting, and, thus, for this analysis we assume that the paleo-stress magnitudes in which the fault system developed were analogous to the contemporary normal faulting stress field in the region. Effective (corrected for fluid pressure) maximum, intermediate and minimum principal stresses (σ_1', σ_2', σ_3') at 5 km depth are estimated to be 90, 65, and 25 MPa (discussed by Morris *et al.*, 1996). We also assumed that the faults

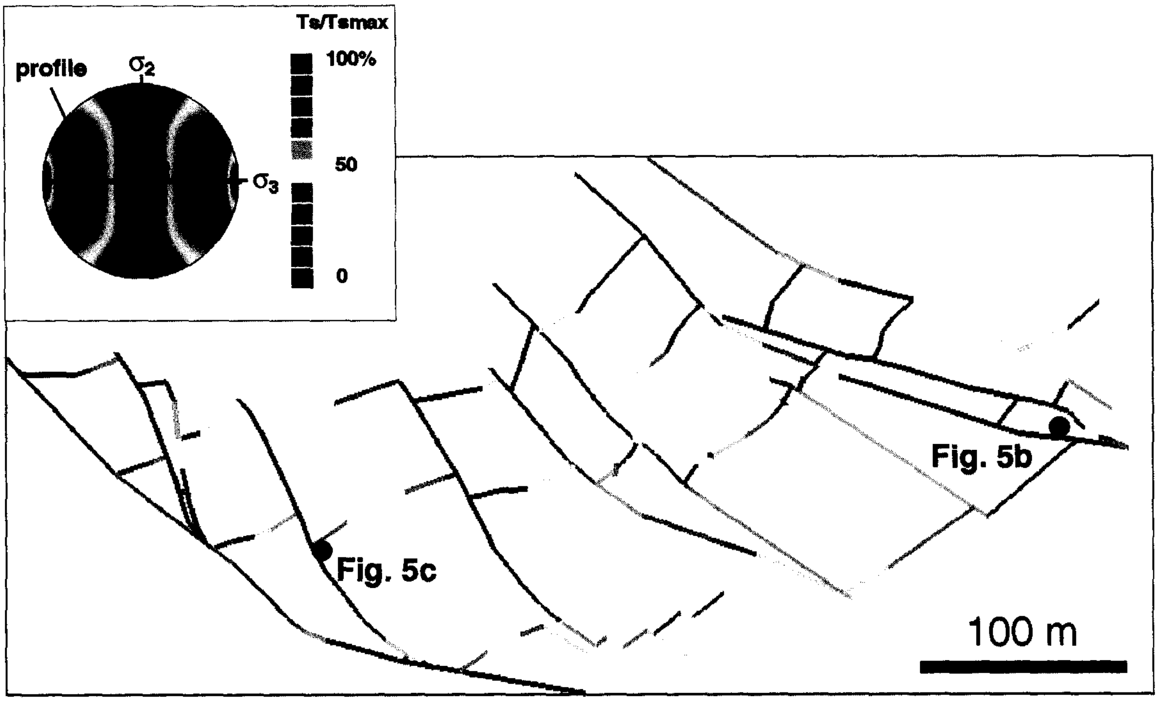

Fig. 6. Slip tendency analysis of a NW–SE cross-section (with no vertical exaggeration) of the fault system (shown in Fig. 4) from Bare Mountain Nevada. The modeled stress field is defined by; $\sigma_1' = 90$ MPa, $\sigma_2' = 65$ MPa and $\sigma_3' = 25$ MPa (after Morris *et al.*, 1996). Note that the slip tendency of faults and bedding are both locally high in the modeled stress field.

originated parallel to the intermediate principal stress, which is typical of normal faulting stress regimes. We expect this stress field to simulate realistically the *pattern* of slip tendency in the fault system, which is the primary focus of this analysis.

The analysis indicates that slip tendency for both faults and bedding was near maximum in parts of the fault system late in development of the system (Fig. 6). This conclusion is consistent with the deformation indicators which show layer-parallel shear deformation synchronous with and subsequent to normal faulting. Thus, this fault system evolved to a point where bedding was appropriately oriented to accommodate a component of the slip and/or shear required for continued extension.

DISCUSSION

The role of fault block rigid rotation vs block deformation by layer-parallel shear is largely governed by material properties of fault block strata. Material yield strength, frictional resistance to sliding and juxtaposition of layers across faults control layer-parallel shear in extensional, imbricate fault systems. Homogeneous isotropic strong fault blocks are likely to rigidly tilt without internal deformation, whereas homogeneous weak fault blocks with a penetrative bedding fabric (anisotropy) are more likely to deform uniformly by layer-parallel shear (Fig. 7). For layer-parallel shear to occur within an inhomogeneous stratigraphic sequence cut by an imbricate normal fault system, two conditions are required. Slip tendency on layering must overcome frictional resistance to sliding and/or yield strength, and relatively weak layers (those poised for slip or shear) must align across faults with similarly poised layers so that slip can be transferred across faults (Figs 5b & 7). Such localized displacement is expected to offset or deflect faults, which in either case will tend to cause resistance to sliding on faults to increase or faults to lock. For a more isotropic sequence of weak strata, shear within the sequence will lower the dip of the host faults, thereby decreasing slip tendency. Extensional layer-parallel shear also decreases bedding cut-off angles and increases down-dip fault length (Fig. 2). In contrast, steeply tilted layers resting on a low-angle fault will result from a strong stratigraphic sequence, or one lacking a strong layering anisotropy, and irregular welded layer contacts, and generally weak faults (compared with layer yield strength and frictional resistance to sliding).

The variation of fault and bedding dips in the Gold Ace Mine exposure produces considerable variation in slip tendency (Fig. 6), suggesting that layer-parallel shear might be expected only in certain fault blocks or parts of fault blocks where slip tendency was highest. Instead, we find evidence of non-uniformly distributed down-dip layer-parallel shear in virtually all fault blocks, even where modeled slip tendency on bedding is low to moderate. Layer-parallel shear is expressed by a variety of structures from penetrative shape fabrics to discrete slip surfaces, which accumulated

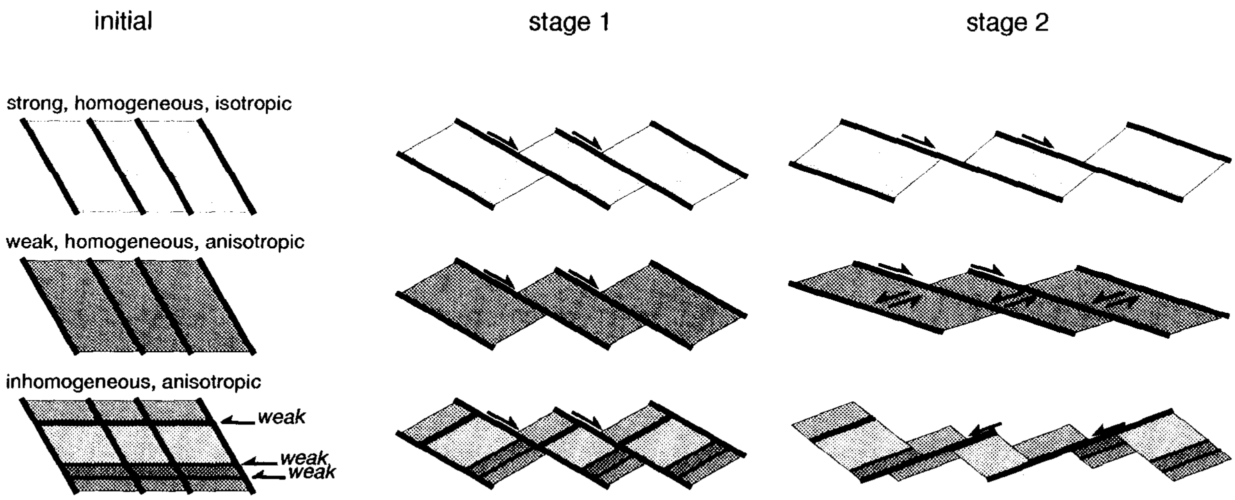

Fig. 7. Schematic model for imbricate fault system evolution in homogeneous isotropic strong, homogeneous anisotropic weak and inhomogeneous anisotropic strata. Layer-parallel shear in an inhomogenous stratigraphic sequence, containing both strong and weak layers, cut by an imbricate normal fault system requires slip tendency on layering in excess of frictional resistance to sliding, and juxtaposition of relatively weak layers (those poised for slip or shear) across faults. Localized shear along bedding is likely to offset faults and cause faults to lock. Homogeneous isotropic strong strata lack planar layering fabric and, therefore, extension is likely to be dominated by fault slip and rigid block rotation which progressively steepens bedding and reduces fault dips. Extensional fault blocks of weak anisotropic strata are more likely initially to deform by layer-parallel shear which tends to reduce bedding dips while fault slip tends to reduce fault dips.

throughout faulting. Although angular shear in some layers is large ($>45^\circ$), fault-bedding cut-off angles have remained high, indicating that bulk layer-parallel shear strain during or after normal faulting was relatively small (Fig. 6). Layer-parallel shear, however, has occurred in gently dipping layering, indicating that layering underwent layer-parallel shear at relatively low slip tendency, and thus was relatively weak. Furthermore, the occurrence of faults offset or deflected by layer-parallel shear indicates that at least some shear occurred during or after the major period of normal faulting.

The protracted history of down-dip shear and its widespread occurrence in fault blocks, even where layer-parallel slip-tendency is low and fault–bedding cut-off angles high, indicates that its development can be attributed to: (1) fault-block shape changes above curved faults resulting from constant bed length and thickness deformation (e.g. Ferrill and Morris, 1997); and (2) bedding-parallel shear initiated as block tilt causes beds to approach orientations with high slip tendencies in the ambient stress field. Localization of shear depends on lithology and the juxtaposition of layers across faults. Competency contrasts at layer boundaries, such as between sandy or silty carbonate beds and limestone, localized slip along discrete surfaces at bed boundaries. Limestone beds accommodated layer-parallel shear by grain-scale ductile flow which deformed primary sedimentary fabrics and early compactional stylolites. Argillaceous limestone beds accomplished shear by grain-scale ductile flow and some component of pressure solution which developed cleavage at low angles to bedding.

CONCLUSIONS

Models of extensional faulting that include significant mechanical contrast within fault blocks predict layer-parallel shear within rotated normal fault blocks. Based on field observations, geometry and stress field configurations, we describe five characteristics of layer-parallel shear in extensional fault systems. (1) Extensional layer-parallel shear is characterized by a down-dip sense of shear, opposite to that observed in contractional structures. (2) Extensional layer-parallel shear is non-uniformly distributed and weak layers or layer boundaries tend to concentrate shear strain, like layer-parallel shear in contractional settings. (3) Increasing extension and steepening of stratal dips in extensional fault blocks tend to increase down-dip layer-parallel shear relative to slip on faults. (4) Increasing extension may rotate faults and fault blocks into orientations that are more favorable for layer-parallel shear and less favorable for fault slip. (5) Extensional layer-parallel shear rotates layering within fault blocks to lower dips. Down-dip layer-parallel shear may be mechanically preferred over fault displacement in highly extended imbricate fault systems. Field observations from Bare Mountain, Nevada, indicate that down-dip layer-parallel shear was an important mechanism of deformation within fault blocks during extensional faulting and may have caused faults to lock.

Acknowledgements—Based on work performed for the U.S. Nuclear Regulatory Commission (Contract NRC-02-93-005). This paper is an independent product of the CNWRA and does not necessarily reflect the views or regulatory position of the NRC. We thank CNWRA reviewers Larry McKague, Bill Dunne and Darrell Sims, and *Journal of Structural Geology* reviewers David Waltham, Wanda Taylor and Peter Hudleston for technical reviews that considerably improved the manuscript. We thank Annette Mandujano for manuscript preparation.

REFERENCES

Anderson, E. M. (1951) *The Dynamics of Faulting and Dyke Formation with Applications to Britain*. Oliver and Boyd, Edinburgh.

Anderson, R. E. (1971) Thin skinned distension in Tertiary rocks of southeastern Nevada. *Bulletin of the Geological Society of America* **82,** 43–58.

Brun, J.-P. and Choukroune, P. (1983) Normal faulting, block tilting, and décollement in a stretched crust. *Tectonics* **2,** 345–356.

Diegel, F. A., Karlo, J. F., Schuster, D. C., Schoup, R. C. and Tauvers, P. C. (1995) Cenozoic structural evolution and tectono-stratigraphic framework of the northern Gulf coast continental margin. In *Salt Tectonics: A Global Perspective*, ed. M. P. A. Jackson, D. G. Roberts and S. Snelson, 65, pp. 109–151. American Association of Petroleum Geologists Memoir.

Dula, W. F., Jr (1990) Geometric models of listric normal faults and rollover folds. *American Association of Petroleum Geologists* **75,** 1609–1625.

Ferrill, D. A. and Dunne, W. M. (1989) Cover deformation above a blind duplex: An example from West Virginia, U.S.A. *Journal of Structural Geology* **11,** 421–431.

Ferrill, D. A. and Morris, A. P. (1997) Geometric considerations of deformation above curved normal faults and salt evacuation surfaces. *The Leading Edge* **16,** 1129–1133.

Ferrill, D. A., Stamatakos, J. A., Jones, S. M., Rahe, B., McKague, H. L., Martin, R. H. and Morris, A. P. (1996a) Quaternary slip history of the Bare Mountain Fault (Nevada) from the morphology and distribution of alluvial fan deposits. *Geology* **24,** 559–562.

Ferrill, D. A., Stamatakos, J. A. and Morris, A. P. (1996b). Structural controls on progressive deformation of the Yucca Mountain (Nevada) Region. *Geological Society of America Abstracts with Programs* **28**, No. 7, A-192.

Ferrill, D. A., Stamatakos, J. A. and McKague, H. L. (1997) Quaternary slip history of the Bare Mountain Fault (Nevada) from the morphology and distribution of alluvial fan deposits: Reply. *Geology* **25,** 190.

Groshong, R. H., Jr (1990) Unique determination of normal fault shape from hanging-wall bed geometry in detached half grabens. *Eclogae Geologica Helvetica* **83,** 455–471.

Higgs, W. G., Williams, G. D. and Powell, C. M. (1991) Evidence for flexural shear folding associated with extensional faults. *Bulletin of the Geological Society of America* **103,** 710–717.

Maldonado, F. (1990) Structural geology of the upper plate of the Bullfrog Hills detachment fault system, southern Nevada. *Bulletin of the Geological Society of America* **102,** 992–1006.

Monsen, S. A., Carr, M. D., Reheis, M. C. and Orkild, P. A. (1992) *Geologic Map of Bare Mountain, Nye County, Nevada*. U.S. Geological Survey Miscellaneous Investigations Series, Map I-2201.

Morris, A. P., Ferrill, D. A. and Henderson, D. B. (1996) Slip tendency analysis and fault reactivation. *Geology* **24,** 275–278.

Proffett, J. M., Jr (1977) Cenozoic geology of the Yerington District, Nevada, and its implications for the nature and origin of Basin and Range faulting. *Bulletin of the Geological Society of America* **88,** 247–266.

Ramsay, J. G. and Huber, M. I. (1987) *The Techniques of Modern Structural Geology, Volume 2: Folds and Fractures*. Academic Press, London.

Rouby, D., Fossen, H. and Cobbold, P. R. (1996) Extension, displacement, and block rotation in the larger Gullfaks area, northern North Sea: Determined from map view restoration. *Bulletin of the American Association of Petroleum Geologists* **80,** 875–890.

Stamatakos, J. A. and Ferrill, D. A. (1996) Kinematic constraints on central Basin and Range tectonism from paleomagnetic and fission track studies at Bare Mountain, Nevada. *Geological Society of America Abstracts with Programs* **28**, No. 7, A-125.

Suppe, J. (1983) Geometry and kinematics of fault-bend folding. *American Journal of Science* **283,** 684–721.

Wernicke, B. and Burchfiel, B. C. (1982) Modes of extensional tectonics. *Journal of Structural Geology* **4,** 105–115.